MHC ligand generation in T cell-mediated immunity and MHC multimer technologies for T cell detection

Bakker, A.H.

Chapter 6

Parallel detection of antigen–specific T–cell responses by multidimensional encoding of MHC multimers

Sine Reker Hadrup*, Arnold H. Bakker*, Chengyi J. Shu, Rikke S. Andersen, Jerre van Veluw, Pleun Hombrink, Emilie Castermans, Per thor Straten, Christian Blank, John B. Haanen, Mirjam H. Heemskerk, and Ton N. Schumacher

Nat Methods. 2009 Jul;6(7):520–6

(* these authors contributed equally to this work)

Parallel detection of antigen-specific T-cell responses by multidimensional encoding of MHC multimers

Sine Reker Hadrup[1,4,5], Arnold H Bakker[1,4,5], Chengyi J Shu[1], Rikke S Andersen[2], Jerre van Veluw[1], Pleun Hombrink[3], Emilie Castermans[1], Per thor Straten[2], Christian Blank[1], John B Haanen[1], Mirjam H Heemskerk[3] & Ton N Schumacher[1]

The use of fluorescently labeled major histocompatibility complex multimers has become an essential technique for analyzing disease- and therapy-induced T-cell immunity. Whereas classical major histocompatibility complex multimer analyses are well-suited for the detection of immune responses to a few epitopes, limitations on human-subject sample size preclude a comprehensive analysis of T-cell immunity. To address this issue, we developed a combinatorial encoding strategy that allows the parallel detection of a multitude of different T-cell populations in a single sample. Detection of T cells from peripheral blood by combinatorial encoding is as efficient as detection with conventionally labeled multimers but results in a substantially increased sensitivity and, most notably, allows comprehensive screens to be performed. We obtained proof of principle for the feasibility of large-scale screening of human material by analysis of human leukocyte antigen A3–restricted T-cell responses to known and potential melanoma-associated antigens in peripheral blood from individuals with melanoma.

T cells recognize virus-infected cells and tumor cells by detecting the presence of disease-specific peptide–major histocompatibility complexes (pMHC) with their clone-specific T-cell receptor. Both for the monitoring of disease-specific immune responses and for the development of new immunotherapeutics, it is essential to specifically detect only those T cells that recognize a given pMHC complex within the large pool of irrelevant T cells[1]. The use of soluble multimeric pMHC complexes to detect such antigen-specific T cells by flow cytometry was first described in 1996 (ref. 2) and has since then become a cornerstone of T-cell monitoring[3]. However, a major limitation in the use of this methodology is that at most, a few antigen specificities can be monitored in a single biological sample because of limitations on the number of available fluorochromes[4].

Prior work has shown that it is feasible to detect antigen-specific T cells by the binding of two different fluorochrome-coded major histocompatibility complex (MHC) multimers containing the same or a related peptide. This technology of double MHC multimer staining has been used to reveal the fine specificity of T cells for variants of single peptide epitopes[5]. If a large set of such dual-color–encoded pMHCs could be combined in a single sample without interfering with the ability of each single pMHC to detect specific T cells, such a technology could conceivably be used to detect a much larger number of T-cell specificities than is currently possible with classical MHC multimer analysis.

Here we demonstrate that a large number of antigen-specific T-cell responses (at least 25) can indeed be analyzed in parallel through the use of pMHC multimers that are each coupled to a unique combination of fluorochromes, with the same fluorescent label being used many times, but in each case in a unique combination with one or more other labels. We exemplify the value of this 'combinatorial encoding' by dissecting melanoma-associated T-cell responses in peripheral blood from individuals with melanoma.

RESULTS

The concept of combinatorial encoding

In this approach, a specific T-cell population is no longer defined by a single fluorescent signal, as is the case in standard MHC multimer stainings, but instead is visualized by the joint binding of multiple fluorochromes. Conceptually, the approach can be considered a self-assembling molecular coding scheme, in which unique codes are only assembled at the moment of T-cell binding (**Fig. 1a**). The power of such a scheme becomes evident with an increasing number of available fluorochromes (**Fig. 1b**). In this study, we explored two-dimensional combinatorial encoding with eight fluorochromes, which deliver 28 unique codes (**Supplementary Table 1**), and demonstrated the ability to expand to three-dimensional combinatorial encoding using the five most intense fluorochromes.

Feasibility of combinatorial encoding

We first determined the feasibility of using six different quantum dots (Qdots) as fluorescent labels for pMHC multimers, in addition

[1]Division of Immunology, The Netherlands Cancer Institute, Amsterdam, The Netherlands. [2]Center for Cancer Immune Therapy, Department of Hematology, Herlev University Hospital, Herlev, Denmark. [3]Department of Hematology, Leiden University Medical Center, Leiden, The Netherlands. [4]Present addresses: Center for Cancer Immune Therapy, Department of Hematology, Herlev University Hospital, Herlev, Denmark (S.R.H.) and Division of Immunology and Pathogenesis, Department of Molecular and Cell Biology, University of California, Berkeley, USA (A.H.B.). [5]These authors contributed equally to this work. Correspondence should be addressed to T.N.S. (t.schumacher@nki.nl).

RECEIVED 6 FEBRUARY; ACCEPTED 28 MAY; PUBLISHED ONLINE 21 JUNE 2009; DOI:10.1038/NMETH.1345

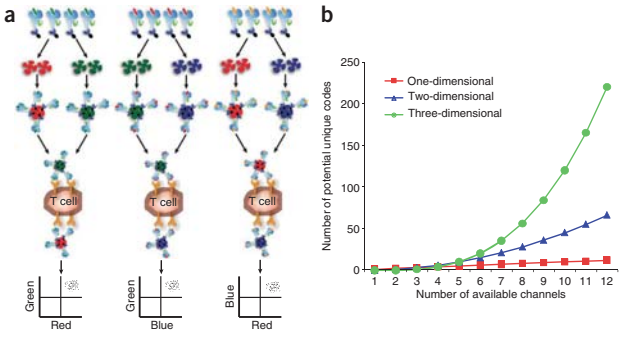

Figure 1 | Overview of the combinatorial encoding approach. (**a**) MHC molecules with different peptide specificities (green, red and orange peptides, top) are conjugated with different fluorochrome color codes (red, green and blue fluorochromes, second row) to generate differentially encoded pMHC multimers (third row). Combinatorial codes are then assembled on T-cell surfaces (fourth row) and these T-cell samples are analyzed by flow cytometry (bottom). (**b**) The theoretical number of unique color combinations that can be made using fluorochromes for the indicated numbers of available channels in either one-, two- or three-dimensional coding schemes.

to allophycocyanin (APC) and phycoerythrin (PE) fluorescent labels (**Supplementary Table 1**), which are more commonly used for the detection of antigen-specific T-cell responses. By analyzing peripheral blood samples for cytomegalovirus (CMV)-specific $CD8^+$ T-cell responses, we established that pMHC complexes that were multimerized by coupling to streptavidin-conjugated Qdots, APC or PE could all be used to detect antigen-specific T cells (**Supplementary Fig. 1**). Subsequently we analyzed whether antigen-specific T-cell populations could reliably be identified by the binding of two pMHC multimers that contain the same antigenic peptide but that are coupled to a different fluorochrome (**Fig. 1a**). Testing of pMHC complexes conjugated to all 28 possible combinations of two different fluorochromes demonstrated that such dual encoding can in all cases reveal the appropriate T-cell population, with only limited variation in detection efficiency between the different color combinations (**Fig. 2a**). As expected, simultaneous staining of T cells with two differentially labeled pMHC multimers that contain the same antigenic peptide leads to a small reduction in fluorescence intensity for each channel (an expected factor of 2 at equimolarity). To limit this negative effect, we used the three Qdots that yielded the lowest intensity signal on our flow cytometric system (Qdots QD565, QD585 and QD800) in a 2:1 rather than 1:1 ratio relative to the other fluorochromes, and we did not use the Qdot combinations QD565 and QD585; QD565 and QD800; and QD585 and QD800 in subsequent experiments, thereby reducing the number of combinations to 25.

Sensitivity of combinatorial encoding

Antigen-specific T-cell populations can be present at very low frequencies, and pMHC multimers do show low-level background staining. To test whether the detection of antigen-specific T cells with combinatorial encoding affects background staining or the frequency of antigen-specific T cells detected, we stained peripheral blood mononuclear cells (PBMCs) containing a low-frequency T-cell response to the human leukocyte antigen (HLA)-A2–restricted CMV epitope NLVPMVATV (CMV-NLV) with HLA-A2 CMV-NLV multimers or with irrelevant HLA-A2 multimers and analyzed them by flow cytometry. Specifically, we incubated PBMCs either with the eight different single-color pMHC multimers in eight separate stainings or with the 25 dual-color–encoded MHC multimers in 25 separate stainings. We considered T cells positive for MHC multimer binding when detected above background either in one channel (for single-color stainings) or when detected in both relevant channels (for dual-color encodings). Notably, the frequency of false positive cells observed upon staining with irrelevant HLA-A2 multimers was approximately tenfold lower when using a dual encoding scheme as compared to the traditional single-staining approach (**Fig. 2b**). This is because most background events are only positive in a single channel and are therefore excluded by combinatorial encoding.

Having established the feasibility of dual-color encoding, we examined whether multiple dual-color–encoded MHC multimer stainings can be performed in parallel on a single sample. To analyze T cells reactive with any of the dual-color–encoded pMHC multimers in a single sample, we developed a gating strategy. In brief, we identified single live $CD8^+$ T cells (**Fig. 2c** and Online Methods) and analyzed T-cell populations reactive with any of the dual-color–encoded pMHC multimers by gating on each of the eight individual fluorochromes used to form the 25 different unique combinations (**Fig. 2c**), as exemplified by gating PE and QD705 double positive $CD8^+$ T cells from both a relevant and an irrelevant mix of pMHC multimers. This strategy identified T cells with signal above background in a given combination of two channels and that are negative in the remaining six channels, thereby allowing the simultaneous analysis of 25 different combinations in one flow cytometry experiment.

Single-sample visualization of up to 25 T-cell responses

We generated 25 different pMHC multimers containing various viral and cancer epitopes for the human MHC alleles HLA-A1, -A2, -A3 and -B7 (**Supplementary Table 2**) by MHC peptide exchange[6–8]. Then, we coupled each of these pMHC multimers to two fluorochromes, generating a set of unique codes (**Supplementary Table 2**). To compare the data obtained by combinatorial encoding with conventional MHC-multimer analysis, we made PE-labeled pMHC multimers in parallel using the same T-cell epitopes. To determine the background of combinatorial encoding, we also prepared irrelevant pMHC multimers in all two-color combinations.

We analyzed PBMCs from three healthy donors covering all four HLA alleles (**Fig. 3a–c**) by (i) one single staining with the mix of dual-color–encoded viral and cancer epitope pMHC multimers, (ii) 25 separate stainings with all individual dual-color–encoded pMHC multimers, (iii) one single staining with the mix of dual-color–encoded irrelevant pMHC multimers or (iv) 25 separate stainings with all 25 PE-labeled pMHC multimers. We performed the experiment in a blinded fashion with respect to HLA haplotype

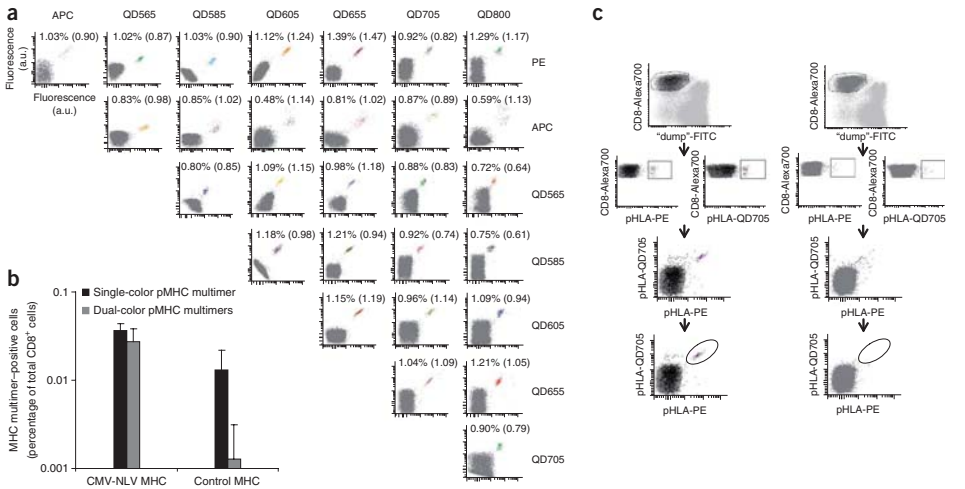

Figure 2 | Feasibility of T-cell staining with dual-color–encoded pMHC multimers. (**a**) Flow cytometry plots displaying fluorescence intensity for the fluorochromes listed at the top and right side of the plot matrix. PBMCs stained using the 28 possible two-color combinations of HLA-A2 CMV-NLV MHC multimers in separate stainings were analyzed, as indicated. Each plot is labeled with the percentage of HLA-A2 CMV-NLV–specific T cells out of total $CD8^+$ cells and, in parentheses, the number of detected HLA-A2 CMV-NLV–specific T cells divided by the average number of HLA-A2 CMV-NLV–specific cells found for all color combinations (average of three experiments using three different donors). Dot plots were gated on approximately 10,000 $CD8^+$ lymphocytes. Gray dots represent $CD8^+$ T cells with no MHC multimer binding, colored dots represent MHC multimer–reactive $CD8^+$ T cells (**b**) Percentage of MHC multimer–positive T cells found with the indicated techniques. Data are mean ± s.d., $n = 25$ for gray bars and $n = 8$ for black bars. (**c**) Schematic overview of the gating strategy used for identification of pMHC-specific T cells after staining with dual-color–encoded MHC multimers. PBMCs were stained with relevant pMHC complexes to visualize antigen-specific T cells (left) or with irrelevant pMHC complexes to indicate background staining (right). $CD8^+$ and 'dump' (FITC) negative cells are selected (dark gray; top). Cells positive in two different MHC multimer channels (PE, QD705) are indicated in purple, and cells positive in any of the other multimer channels indicated in black (second row). Then one determines whether cells are double positive for the two selected colors (third row). Cells positive in three or more MHC multimer channels are removed (bottom). In typical final data plots, an antigen-specific T-cell population is indicated by fluorescence in two defined channels (bottom, left).

and to prior analysis of antigen-specific T-cell responses in these donors. Combinatorial encoding of pMHC multimers allowed the simultaneous visualization of a large number of antigen-specific T-cell populations in one single sample (**Fig. 3** and **Supplementary Fig. 2**). Notably, we found the same virus-specific T-cell populations in each donor when analyzed by individual PE-multimer stainings. Furthermore, statistical comparison between staining strategies i, ii and iv revealed a high interclass correlation (interclass correlation coefficient (ρ) = 0.84 (95% confidence interval: 0.78–0.89)), describing an almost perfect agreement between the outcomes of the three strategies[9]. Individual comparison between the mix of 25 dual-color–encoded pMHC multimers in one sample (strategy i) with either the PE-tetramer stainings (strategy iv) or the same set of dual-color–encoded pMHC multimers in 25 separate stainings (strategy ii) reveal similarly high correlations ($\rho = 0.79$ (95% confidence interval: 0.68–0.86) and $\rho = 0.83$ (95% confidence interval: 0.74–0.89), respectively) (**Fig. 4**). Thus, the simultaneous detection of multiple antigen specificities with sets of pMHC multimers, in which each multimer is coupled to a distinct combination of fluorochromes, is feasible. Finally, comparison of the signals from the dual-color–encoded pMHC set containing virus and tumor-associated epitopes (strategy i) with the signals from the pMHC set containing 25 irrelevant MHC multimers (strategy iii) indicates that the sensitivity of the approach is high and that T-cell populations as infrequent as 0.02% of $CD8^+$ cells can be identified (**Figs. 3a–c** and **4a**) (average background: 0.0012% of $CD8^+$ T cells, s.d. = 0.0035, $n = 100$).

To validate the T-cell responses observed by MHC multimer staining using a non–flow cytometry–based method, we performed an INFγ enzyme–linked immunosorbent spot (ELISPOT) assay with these PBMCs using the same 25 peptides (**Fig. 3a–c**). All T-cell responses detected by MHC multimer analysis were confirmed by detection of INFγ secretion. Note that the magnitude of T-cell responses, as measured by INFγ secretion, was in some cases substantially lower than that measured by any of the MHC multimer approaches, consistent with the observation that a variable fraction of antigen-specific T cells acquires the capacity to secrete effector cytokines.

To provide proof of principle for higher-dimension encoding of antigen-specific T-cell responses, we generated eight different combinations of five high-intensity fluorochromes (PE, APC, QD605, QD655 and QD705), in which each antigen specificity was encoded by a unique combination of three different fluorochromes. Even though the frequency of antigen-specific T cells detected was lower as compared to two-dimensional encoding (0.29% versus 0.47% of $CD8^+$ T cells), identification of CMV-NLV–specific T cells in healthy donor PBMCs was feasible using this three-dimensional encoding strategy (**Supplementary Fig. 3**).

Finally, combinatorial encoding can be combined with single-color antibody staining to determine the phenotype of pMHC-specific T cells. To illustrate this, we analyzed the phenotype of three virus-specific T-cell populations, HLA-A2 Inf-GIL, CMV-NLV and EBV-GLC. As described previously[10,11], HLA-A2 CMV-NLV–specific T cells displayed a more differentiated phenotype ($CD45RA^+$, $CCR7^-$, $CD62L^-$ and $CD57^+$ or $CD57^-$), as compared to HLA-A2 EBV-GLC and Inf-GIL T-cell populations

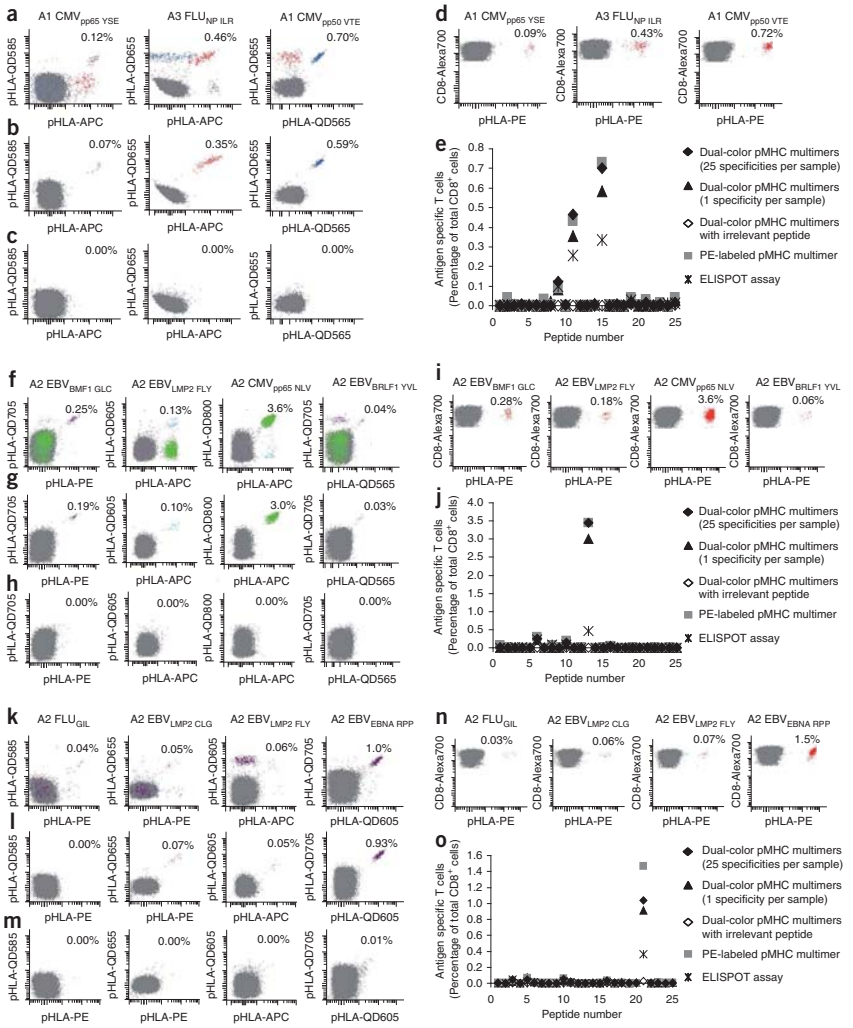

Figure 3 | Multiplex detection of virus-specific T-cell responses through combinatorial encoding. (**a**–**e**) Donor 1. (**f**–**j**) Donor 2. (**k**–**o**) Donor 3. Dot plots of antigen-specific T-cell populations detected at a frequency >0.03% are shown by staining one sample with a mix of 25 different dual-color pMHC multimers (**a**,**f**,**k**); by staining 25 individual samples with 1 of the 25 dual-color pMHC multimers (**b**,**g**,**l**); by staining one sample with a mix of 25 irrelevant dual-color pMHC multimers (**c**,**h**,**m**); and by staining 25 individual samples with classical PE-labeled pMHC multimers each containing one of the 25 peptides (**d**,**i**,**n**). All dot plots are shown with bi-exponential axes and display fluorescence intensity (a.u.) for the fluorochrome indicated on each axis. Graphical representation of the frequency of antigen-specific $CD8^+$ T cells directed against the 25 epitopes (**Supplementary Table 2**), when measured using the four different flow cytometry–based strategies shown in **a**–**d**, **f**–**l** and **k**–**n**, and IFNγ ELISPOT assay(**e**,**j**,**o**).

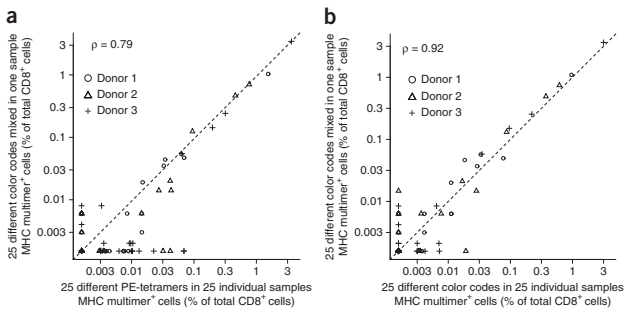

Figure 4 | Correlation between different T-cell detection strategies. (**a**) Correlation between antigen-specific T-cell frequencies as detected by classical PE-labeled MHC multimer staining and by dual-color–encoded MHC multimer staining with 25 specificities per sample. (**b**) Correlation between antigen-specific T-cell frequencies as detected by dual-color–encoded MHC multimers with one pMHC specificity per sample and by dual-color–encoded MHC multimer staining with 25 specificities per sample. Donors are the same as in **Figure 3**. ρ, interclass correlation coefficient. For transforming to logarithmic scale all zero values were converted to 0.0015. Dashed lines represent the optimal linear correlation.

detected in the same sample (CD45RA$^+$ or CD45RA$^-$, CCR7$^-$, CD62L$^-$ and CD57$^-$) (**Supplementary Fig. 4**).

Identification of melanoma-associated T-cell epitopes

Having established the feasibility of combinatorial encoding for the parallel measurement of a large number of antigen-specific T-cell populations in a single sample, we next determined the potential value of combinatorial encoding in epitope identification. In a recent screen[8], we had identified 22 peptides from four different melanoma-associated proteins that display a high affinity for HLA-A3 (**Supplementary Table 3**). This set included all four previously described HLA-A3–associated epitopes as well as 18 potential new epitopes. To address the feasibility of screening small patient samples for responses to sets of potential epitopes, we generated MHC reagents by UV-light–induced peptide-exchange reactions[6–8] for all 22 epitopes, as well as for three HLA-A3–associated Epstein-Barr virus (EBV)-derived and influenza A–derived epitopes, and we encoded these reagents to form fluorescently labeled pMHC multimers as described in **Supplementary Table 3**. Subsequently, we screened

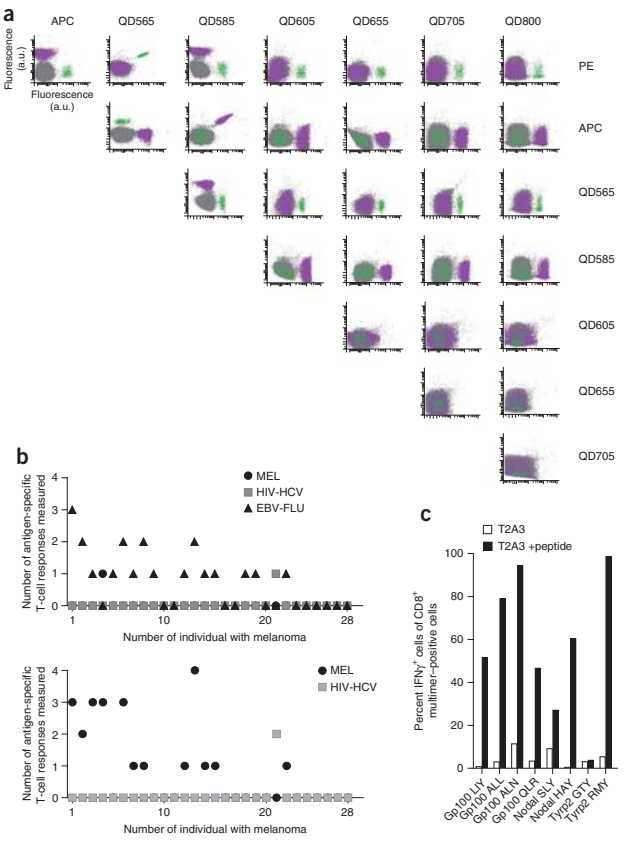

Figure 5 | T-cell responses to melanoma-associated peptides. (**a**) Dot plots show a representative example of pMHC multimer–enriched PBMCs from an individual with melanoma analyzed by combinatorial encoding. Antigen-specific T-cell populations were detected for gp100-LIY (PE and QD565) (green) and Nodal-SLY (APC and QD585) (pink). All dot plots are shown with bi-exponential axes and display fluorescence intensity (a.u.) for the indicated fluorochromes. (**b**) Summary of antigen-specific T-cell responses of 28 individuals to 22 melanoma-associated peptides (MEL), 20 HIV- and HCV-derived T-cell epitopes (HIV-HCV) and three HLA-A3–restricted virus-derived T-cell epitopes (EBV-FLU). The response of each individual is shown for detection directly *ex vivo* (top) and after enrichment and *in vitro* expansion (bottom). (**c**) T-cell cultures (from different individuals) that responded to the indicated peptide in an intracellular IFNγ staining assay. Assays were performed on sorted pMHC multimer–reactive T-cell populations incubated with T2-A3 cells pulsed with or without the indicated peptide. Data from representative cultures are shown for each epitope.

PBMCs from 28 HLA-A3–positive individuals with melanoma for T-cell responses to these potential antigens, either directly *ex vivo* or after antigen-specific T-cell enrichment. In the latter case, we only performed enrichments with pMHC multimers containing melanoma-associated antigens, to avoid potential overgrowth of virus-specific T cells during culture. As expected, we detected EBV- and influenza A–specific responses in the majority (15 out of 28) of the individuals with melanoma directly *ex vivo*. Additionally, we detected a single melanoma-associated antigen-specific response directly *ex vivo*. Notably, using parallel MHC multimer staining, we detected many T-cell responses specific for different potential melanoma-associated antigens after enrichment (**Fig. 5a**). In total, we detected 24 responses targeting eight distinct epitopes (**Fig. 5b**). Three of these epitopes consisted of previously described gp100-derived peptides that have been shown to be presented by tumor cells[12–14]. In addition, we observed responses to five previously unknown T-cell epitopes from gp100 (QLRALDGGNK), Nodal (SLYRDPLPR and HAYIQSLLK) and Tyrp2 (GTYEGLLRR and RMYNMVPFF). In all cases, we confirmed peptide specificity of the T cells with subsequent analysis by conventional MHC multimer staining followed by MHC tetramer–based sorting. We assayed the functional activity of these T-cell populations by measuring IFNγ production upon incubation with peptide-loaded T2-A3 target cells; we confirmed the functional activity of 18 out of 22 cultures analyzed and for four out of the five newly identified epitopes (**Fig. 5c**). We performed the same type of combinatorial encoding analysis using HIV- and hepatitis C virus (HCV)-derived peptides (**Supplementary Table 4**), antigens to which the group of individuals we tested has presumably not been exposed. In these analyses, a sample from only one individual with melanoma showed reactivity against HCV-derived epitopes (HCV-GVA and GCV-KVF) (**Fig. 5b**). Although we could not attribute this single response to a known HCV exposure, the lack of T-cell responses against any of the other viral antigens in these individuals with melanoma suggests that the frequent detection of T-cell responses to the HLA-A3–restricted melanoma-associated antigens in this cohort is a consequence of disease state. Although it remains to be established whether T-cell responses against these antigens can contribute to tumor control, these data make a strong case for the value of combinatorial encoding in epitope identification.

DISCUSSION

With regard to the technical aspects of our approach, three points are noteworthy. First, the use of differentially labeled pMHC complexes carrying the same peptide led to a reduction in signal in each individual channel owing to competition for available binding sites, but such competition is apparently not a major factor. In a setup that used eight channels for encoding, we detected a signal that was clearly discernable above background for 25 out of 28 possible two-dimensional combinations. Based on these data, it seems plausible that with additional improvements in flow-cytometric detection, multiplex analysis will be possible for most or all potential combinations of fluorochromes even when moving to higher-dimension encoding. Second, the sensitivity of detection of antigen-specific T-cell responses by combinatorial encoding is as high or higher than that of classical MHC multimer staining. Background staining in MHC-based detection of T-cell responses can generally be attributed to interaction of cells with a single fluorescent marker or because of random interaction with all fluorescent markers used. Thus, by restricting detection to those T cells that interact with a defined combination of two and only two of the fluorochromes used for encoding, such background events are effectively removed. Finally, a potentially serious issue with the use of combinatorial encoding is the fact that T cells are considered highly cross-reactive. As an example, if CMV-specific T cells would show a spurious cross-reactivity with any of the other pMHC complexes used, such T cells would be detected in more than two channels and thereby be excluded from analysis. Notably, for all antigen-specific T-cell responses that we analyzed in parallel by combinatorial encoding and classical MHC multimer staining, there was a full match between the antigen-specific T-cell populations detected by the two assays and the correlation between the assays was high. Thus, when using sets of dozens of unrelated pMHC multimers, a possible cross-reactivity of T cells appears not to be a measurable factor. We note that such cross-reactivity can be expected to become a relevant issue in the case of high-throughput analysis of T-cell responses with sets of pMHC multimers with substantial structural homology, for instance, involving peptide variants.

Prior work in animal models has demonstrated the value of MHC-based detection of T-cell responses using large sets of pMHC multimers by conventional single-channel analysis. Specifically, for all four tested pathogens (H5N1 influenza A, *Chlamydia trachomatis*, MHV-68 and *Toxoplasma gondii*[6,15–17]), new epitopes had been identified in screens using 150–2,000 peptides. Notably, if the same screens were to be performed on human PBMCs, this would require approximately 300 ml to 4 l of peripheral blood. However, with the ability to analyze at least 25 antigen specificities per sample, this is reduced to substantially more realistic amounts. As a first demonstration of the potential value of large-scale screening of human T-cell responses, we analyzed cytotoxic T-cell responses to potential melanoma-associated antigens. Based on these data, it seems likely that MHC-based detection of T-cell responses will be of substantial value for large-scale screening efforts aimed at the identification of pathogen-, cancer- or autoimmune-associated epitopes. In addition, multiplexed measurement of antigen-specific immune responses could form a useful addition to current analyses of bulk T-cell frequencies in routine human diagnostics.

METHODS

Methods and any associated references are available in the online version of the paper at http://www.nature.com/naturemethods/.

Note: Supplementary information is available on the Nature Methods website.

ACKNOWLEDGMENTS

We thank B. Rodenko and H. Ovaa (Netherlands Cancer Institute) for the kind gift of J, W. van de Kasteele for help with cell culture, T. Wirenfeldt for statistical assistance, and A. Pfauth, F. van Diepen, M. van der Hoorn and G. de Roo for technical support with flow cytometry. This work was supported by the Danish Cancer Society grant DP06031 and the Carlsberg Foundation grant 2005-1-641 (to S.R.H.), Landsteiner Foundation of Blood Transfusion research grant 0522 and a Melanoma Research Alliance established investigator award (to T.N.S.) and Dutch Cancer Society grant UL 2007-3825 (to M.H.H. and T.N.M.S.).

AUTHOR CONTRIBUTIONS

S.R.H., A.H.B. and C.J.S. designed research, performed research, analyzed data and wrote the paper; R.S.A. performed research and analyzed data; J.v.V. performed research; P.H. and E.C. provided practical assistance; P.t.S., C.B. and J.B.H. contributed material from individuals with melanoma; M.H.H., designed research and analyzed data; T.N.S., designed research, analyzed data and wrote the paper.

COMPETING INTERESTS STATEMENT
The authors declare competing financial interests: details accompany the full-text HTML version of the paper at http://www.nature.com/naturemethods/.

Published online at http://www.nature.com/naturemethods/
Reprints and permissions information is available online at http://npg.nature.com/reprintsandpermissions/

1. Arstila, T.P. *et al.* A direct estimate of the human alphabeta T cell receptor diversity. *Science* **286**, 958–961 (1999).
2. Altman, J.D. *et al.* Phenotypic analysis of antigen-specific T lymphocytes. *Science* **274**, 94–96 (1996).
3. Bakker, A.H. & Schumacher, T.N. MHC multimer technology: current status and future prospects. *Curr. Opin. Immunol.* **17**, 428–433 (2005).
4. Chattopadhyay, P.K. *et al.* Quantum dot semiconductor nanocrystals for immunophenotyping by polychromatic flow cytometry. *Nat. Med.* **12**, 972–977 (2006).
5. Haanen, J.B., Wolkers, M.C., Kruisbeek, A.M. & Schumacher, T.N. Selective expansion of cross-reactive CD8(+) memory T cells by viral variants. *J. Exp. Med.* **190**, 1319–1328 (1999).
6. Toebes, M. *et al.* Design and use of conditional MHC class I ligands. *Nat. Med.* **12**, 246–251 (2006).
7. Rodenko, B. *et al.* Generation of peptide-MHC class I complexes through UV-mediated ligand exchange. *Nat. Protoc.* **1**, 1120–1132 (2006).
8. Bakker, A.H. *et al.* Conditional MHC class I ligands and peptide exchange technology for the human MHC gene products HLA-A1, -A3, -A11, and -B7. *Proc. Natl. Acad. Sci. USA* **105**, 3825–3830 (2008).
9. Landis, J.R. & Koch, G.G. The measurement of observer agreement for categorical data. *Biometrics* **33**, 159–174 (1977).
10. Appay, V. *et al.* Memory $CD8^+$ T cells vary in differentiation phenotype in different persistent virus infections. *Nat. Med.* **8**, 379–385 (2002).
11. Appay, V., van Lier, R.A., Sallusto, F. & Roederer, M. Phenotype and function of human T lymphocyte subsets: consensus and issues. *Cytometry A* **73**, 975–983 (2008).
12. Kawakami, Y. *et al.* Identification of new melanoma epitopes on melanosomal proteins recognized by tumor infiltrating T lymphocytes restricted by HLA-A1, -A2, and -A3 alleles. *J. Immunol.* **161**, 6985–6992 (1998).
13. Kawashima, I. *et al.* Identification of gp100-derived, melanoma-specific cytotoxic T-lymphocyte epitopes restricted by HLA-A3 supertype molecules by primary in vitro immunization with peptide-pulsed dendritic cells. *Int. J. Cancer* **78**, 518–524 (1998).
14. Skipper, J.C. *et al.* Shared epitopes for HLA-A3–restricted melanoma-reactive human CTL include a naturally processed epitope from Pmel-17/gp100. *J. Immunol.* **157**, 5027–5033 (1996).
15. Frickel, E.M. *et al.* Parasite stage-specific recognition of endogenous Toxoplasma gondii-derived CD8+ T cell epitopes. *J. Infect. Dis.* **198**, 1625–1633 (2008).
16. Gredmark-Russ, S., Cheung, E.J., Isaacson, M.K., Ploegh, H.L. & Grotenbreg, G.M. The CD8 T-cell response against murine gammaherpesvirus 68 is directed toward a broad repertoire of epitopes from both early and late antigens. *J. Virol.* **82**, 12205–12212 (2008).
17. Grotenbreg, G.M. *et al.* Discovery of CD8+ T cell epitopes in Chlamydia trachomatis infection through use of caged class I MHC tetramers. *Proc. Natl. Acad. Sci. USA* **105**, 3831–3836 (2008).

ONLINE METHODS

Generation of pMHC complexes. All peptides were synthesized in-house using standard Fmoc chemistry or purchased from Pepscan (Pepscan Presto BV). The UV light–sensitive building block J was synthesized as described[6–8]. Recombinant HLA-A1, -A2, -A3 and -B7 heavy chains and human β_2m light chain were produced in *Escherichia coli*. MHC class I refolding reactions were performed as described[18] and MHC class I complexes were purified by gel-filtration high-performance liquid chromatography in PBS (pH 7.4). Specific peptide-MHC complexes were generated by MHC peptide exchange[6–8]. In brief, UV light–sensitive pMHC complexes (100 μg ml^{-1}) were subjected to 366 nm UV light (Camag) for 1 h in presence of the various peptides (200 μM). After exchange, samples were centrifuged at 16,000*g* for 5 min, and supernatants were used for pMHC multimer formation.

Generation of pMHC multimers. pMHC multimers were generated using eight different fluorescent streptavidin (SA) conjugates (Invitrogen): SA-QD565, SA-QD585, SA-QD605, SA-QD655, SA-QD705, SA-QD800, SA-PE and SA-APC. For each 100 μl of MHC monomer (concentration, 100 μg ml^{-1}) 7.08 μl of SA-Qdot conjugate (1 μM), 10.8 μl SA-PE (1 mg ml^{-1}) or 6 μl SA-APC (1 mg ml^{-1}) was added, followed by incubation on ice for 20 min. Assuming a 100% rescue after MHC peptide exchange, this would result in an occupancy of 30 MHC monomers per SA-Qdot and 4 monomers per SA-PE or SA-APC. To block residual binding sites, D-biotin (Sigma) was added to a final concentration of 26.4 μM, followed by incubation on ice for 20 min. PE- and APC-labeled complexes were diluted twofold in PBS with 0.02% (wt/vol) NaN_3. For each pMHC complex, multimers were made with two different fluorescent labels according to the schemes in **Supplementary Tables 2–4**. For combinatorial T-cell staining, multimer complexes of the same specificity were mixed 1:1 for QD605-, QD655-, QD705-, PE- and APC-labeled complexes and 2:1 for QD565-, QD585- and QD800-labeled complexes in combination with any other color. Combinations of QD565, QD585 and QD800 with each other were excluded. Combined pMHC mixtures for analysis of T-cell responses by combinatorial encoding were generated by pooling and were stored with 0.02% NaN_3 (Sigma) at 4 °C as 50-fold concentrated ready-to-use stocks for T-cell staining (concentration was 100 μg ml^{-1} based on initial monomer concentration). Before use, pMHC multimers were centrifuged at 17,000*g* for 2 min, and the supernatant was used. Although the stability of pMHC complexes can be expected to differ between individual pMHC complexes, we have successfully used pMHC mixtures stored in this manner for up to 2 months.

PBMC samples and T-cell staining. PBMCs were obtained from healthy individuals and from individuals with stage IV melanoma in accordance with local guidelines, with informed consent and with approval from the local ethics committee (METC). All T-cell staining was performed on cryopreserved material. For T-cell staining of approximately 1×10^6 PBMCs or 2×10^5 cultured T cells, 2 μl of single pMHC multimer, or 50 μl of dual-color–encoded pMHC collections (final concentration: 2 μg ml^{-1} per distinct pMHC based on initial monomer concentration) was used. Final staining volume was 80 μl and cells were incubated for 10 min at 37 °C. Next, 20 μl of a fivefold concentrated antibody mix consisting of CD8-Alexa700 (Caltag MHCD0829) (final dilution 1/200), CD4-FITC (BD 345768) (final dilution 1/8), CD14-FITC (BD 345784) (final dilution 1/32), CD19-FITC (BD 345776) (final dilution 1/16), CD40-FITC (Serotech MCA1590F) (final dilution 1/40), CD16-FITC (BD 347523) (final dilution 1/64) was added, and cells were incubated for 20–30 min at 4 °C. Before flow cytometry analysis, cells were washed twice and propidium iodide was added to allow dead-cell exclusion.

Flow cytometry. Data acquisition was performed on an LSR-II flow cytometer (Becton Dickinson) with FacsDiva software using the following 11-color instrument settings. For the 488-nm laser: PI, 685LP, 695/40; PE, 550LP, 575/26; FITC, 505LP, 530/30; SSC, 488/10. For the 633-nm laser: Alexa700, 685LP, 730/45; APC, 660/20. For the 405-nm laser: QD800, 770LP, 800/30; QD705, 680LP, 710/50; QD655, 635LP, 660/40; QD605, 595LP, 650/12. For the 355-nm laser: QD585, 575LP, 585/15; QD565, 545LP: 560/20. Approximately 200,000 lymphocytes were recorded for each analysis. To identify antigen-specific T cells, the following gating strategy was used. (i) Selection of live (PI-negative) single-cell lymphocytes (FSC-W/H low, SSC-W/H low, FSC/SSC-A). (ii) Selection of CD8$^+$ and 'dump' (CD4, 14, 16, 19 and 40) negative cells. FITC was used as a 'dump channel' to gate away all irrelevant cells, as a means to reduce background[19]. (iii) Selection of CD8$^+$ T cells that were positive in two MHC multimer channels and negative in the six other MHC multimer channels. Each cell population positive in two and only two MHC multimer channels received a unique color to facilitate analysis.

IFNγ enzyme-linked immunosorbent spot assay. We coated 96-well nitrocellulose plates (Multiscreen MAIP N45; Millipore) with 7.5 μg ml^{-1} mouse monoclonal antibody to IFNγ (1-D1k; Mabtech) in 75 μl PBS overnight at room temperature. After six washes and blocking with 200 μl X-Vivo medium (Biowhittaker), lymphocytes were added in three concentrations: 1×10^6, 5×10^5 and 2.5×10^5 cells per well, together with indicated peptide (5 μg ml^{-1}). After overnight incubation, plates were washed and biotinylated secondary monoclonal antibody to IFNγ was added (7-B6-biotin; Mabtech). After a 2-h incubation, plates were washed and avidin-enzyme conjugate (Life Technologies) was added to each well. After 1 h of incubation at room temperature, plates were washed and enzyme substrate (Dako) was added for 5–10 min. Reactions were terminated by addition of water, and the number of spots was assessed using an ELISPOT counter (Immunospot; CTL Inc.).

Enrichment of antigen-specific T cells. Antigen-specific T cells were stained with PE multimers (1.25 μl of a 100 μg ml^{-1} stock of each individual PE-multimer for 10^7 PBMCs) for 1 h at 4 °C. Subsequently, cells were washed, and incubated with 20 μl magnetic beads coated with antibody to PE (Miltenyi). Cells were then isolated by MACS (Miltenyi), using an LS column, following the manufacturer's protocol. Eluted cells were washed and resuspended in 200 μl of T cell medium (IMDM (Gibco) with 10% human serum (Invitrogen), 100 IU ml^{-1} IL-2 (Proleukin) and 20 ng ml^{-1} IL-15 (Peprotech)) with 5,000 anti-CD3/CD28–coated Dynabeads (Invitrogen). Enriched cells were cultured in 96-well plates and resuspended the next day. Cultures were split and medium was refreshed at least twice a week. Note that residual PE-multimer staining from the enrichment step disappears

within two days of culture (data not shown). After 2–3 weeks, antigen-specific T-cell responses were measured by combinatorial encoding-based MHC multimer flow cytometry.

T-cell sorting and culture. T cells were stained with the relevant pMHC multimer and then sorted on a MoFlo (Dako) or FACSAria (Becton Dickinson) into 10^5 irradiated feeder cells (JY plus allogeneic PBMCs). Cells were spun and resuspended in IMDM with 10% human serum, 100 IU ml^{-1} IL-2 and 0.5 μg ml^{-1} PHA (Biochrom AG). Cultures were restimulated every second week. Established cultures were tested for antigen-specificity by MHC multimer staining.

Cytokine release assay. T2-A3 cells were loaded with the indicated peptides for 1 h and washed once. Then, 1×10^5 T cells from indicated cultures were incubated with 1×10^5 T2-A3 cells for 4 h at 37 °C in IMDM with 10% human serum and protein transport inhibitor (BD GolgiPlug). Cells were stained with PE-conjugated antibodies to CD8 (clone SK1, BD) for 15 min at 25 °C, fixed and permeabilized (BD Cytofix/Cytoperm kit), and stained with APC-conjugated antibodies to IFNγ (25723.11, BD) for 30 min at 4 °C. Samples were analyzed by flow cytometry (Cyan, Dako), data analysis was performed using FlowJo.

Statistics. The three different staining approaches: (i) one single staining with the mix of 25 dual-color–encoded viral and cancer epitope pMHC multimers, (ii) 25 separate stainings with all 25 PE-labeled pMHC multimers or (iii) 25 separate stainings with all individual dual-color–encoded pMHC multimers were compared to determine the interclass correlation, using a two-way mixed model (ICC3.1), calculated based on consistency. Interpretation of the results is based on reference 9.

18. Garboczi, D.N., Hung, D.T. & Wiley, D.C. HLA-A2–peptide complexes: refolding and crystallization of molecules expressed in *Escherichia coli* and complexed with single antigenic peptides. *Proc. Natl. Acad. Sci. USA* **89**, 3429–3433 (1992).
19. van Oijen, M. *et al.* On the role of melanoma-specific CD8+ T-cell immunity in disease progression of advanced-stage melanoma patients. *Clin. Cancer Res.* **10**, 4754–4760 (2004).

SUPPLEMENTARY INFORMATION

Supplementary Figure 1

Detection of antigen–specific T cells using MHC multimers coupled to different fluorochromes

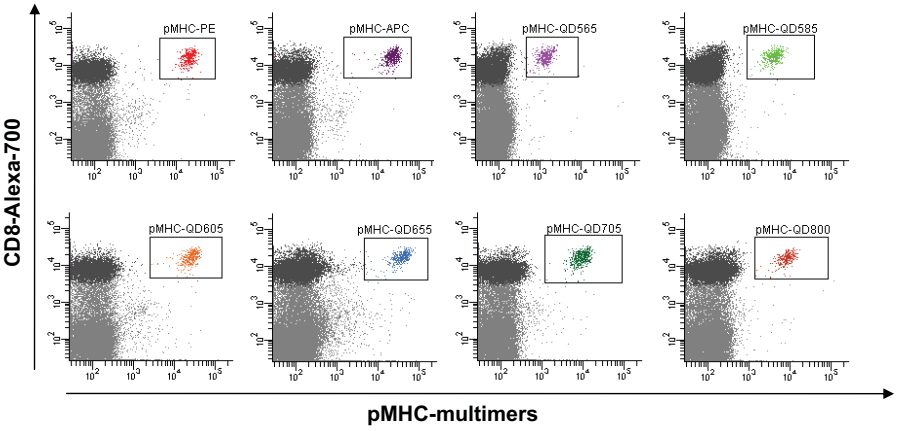

Staining of a clonal HLA–A2 CMV_{NLV}–specific T cell population mixed with an excess of HLA–A2–negative PBMCs using MHC multimers conjugated to eight different fluorochromes: PE, APC, QD565, QD585, QD605, QD655, QD705 and QD800. Dot plots are gated on live, single–cell lymphocytes.

Supplementary Figure 2

Multiplex detection of virus–specific T cell responses through combinatorial encoding

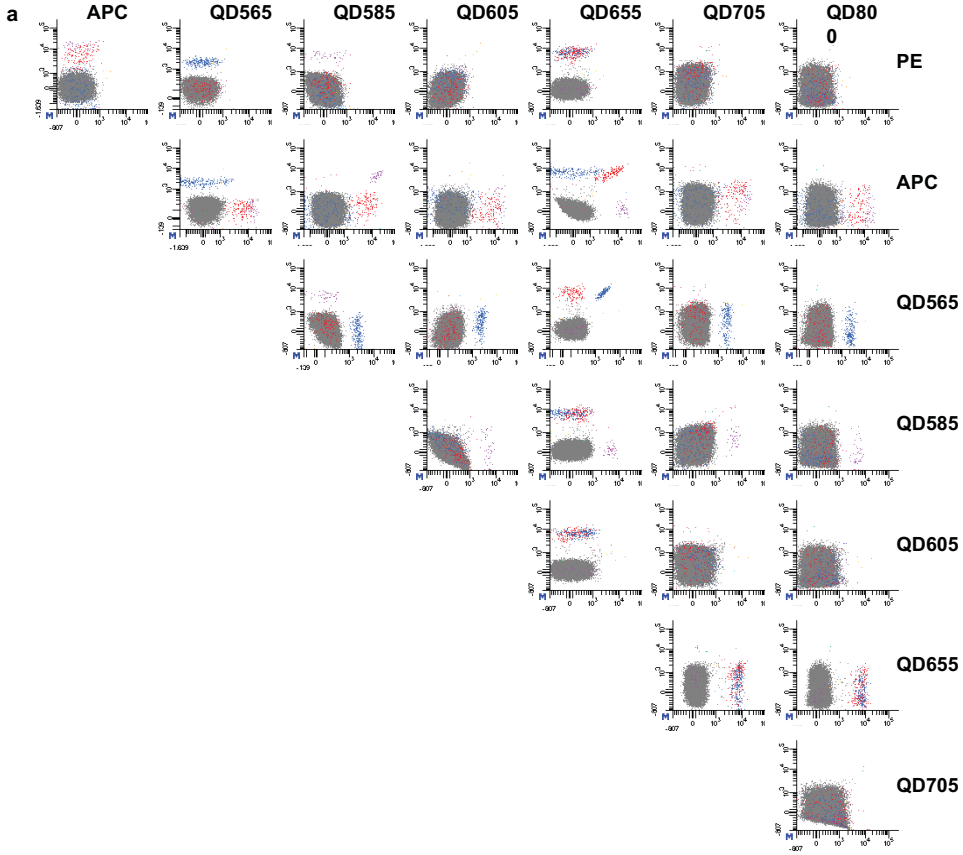

(**a–c**) Dot plots showing all 28 different 2–D representations of gated $CD8^+$ T cells of three healthy donors analyzed by dual–color encoded MHC multimer staining using the peptide set described in **Supplementary Table 2** online. (**a**) Donor 1. (**b**) Donor 2. (**c**) Donor 3. (**d**) Representative example of staining of PBMCs from a healthy donor analyzed by dual–color encoded MHC multimer staining using irrelevant peptide–MHC multimers. (**e**) Dot plots for healthy donor 2 gated on all lymphocytes.

Supplementary Figure 2

Multiplex detection of virus–specific T cell responses through combinatorial encoding

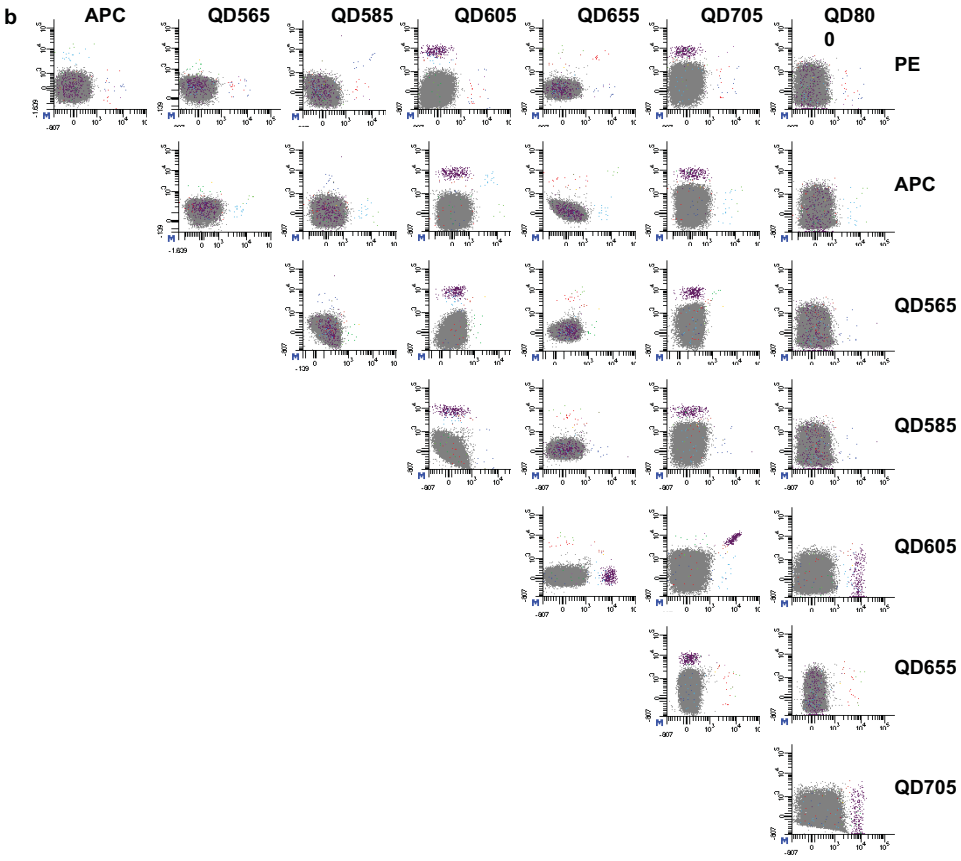

Supplementary Figure 2

Multiplex detection of virus–specific T cell responses through combinatorial encoding

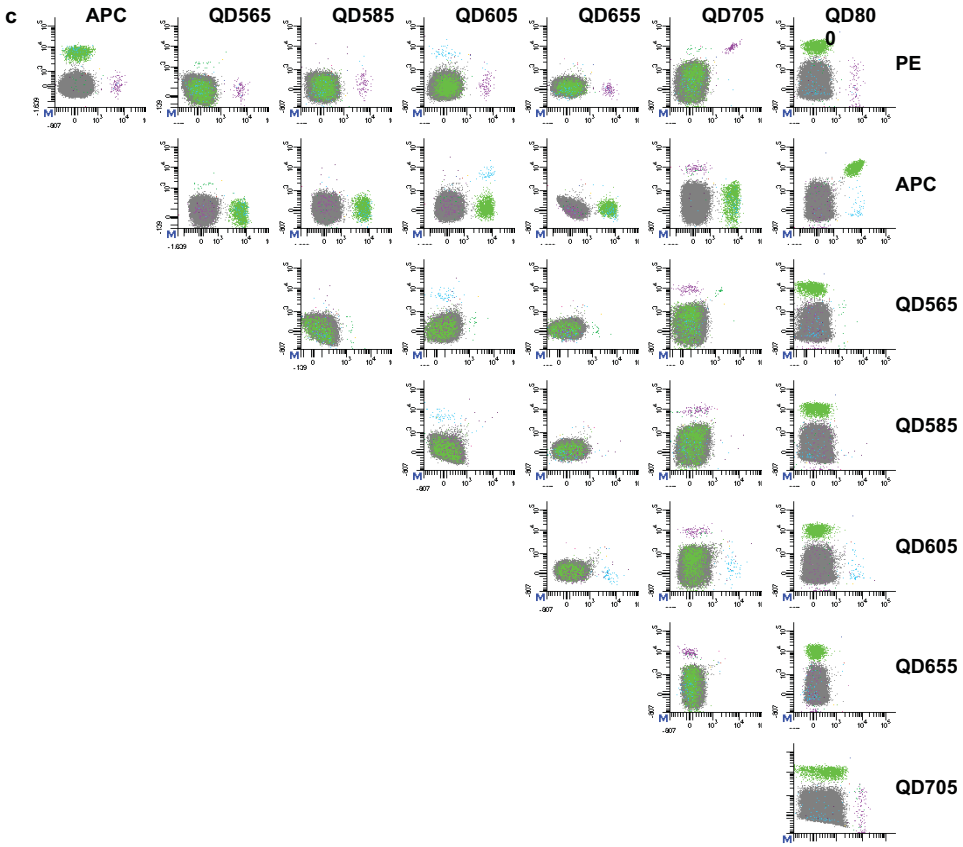

Supplementary Figure 2

Multiplex detection of virus–specific T cell responses through combinatorial encoding

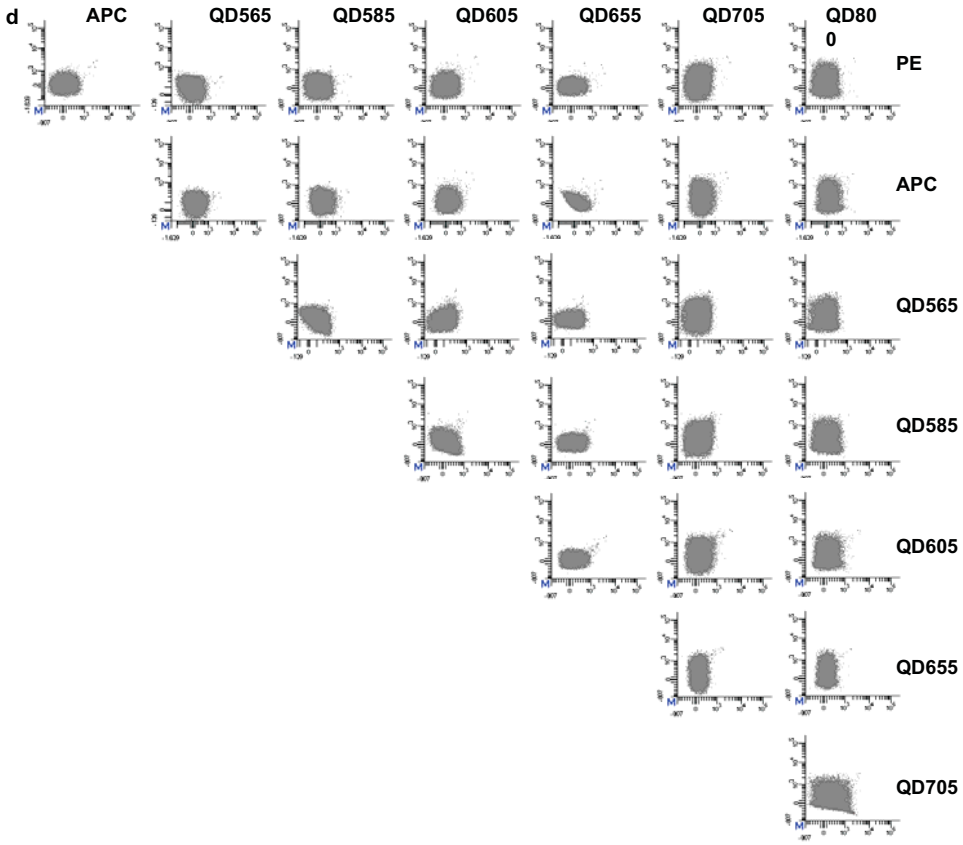

Supplementary Figure 2

Multiplex detection of virus–specific T cell responses through combinatorial encoding

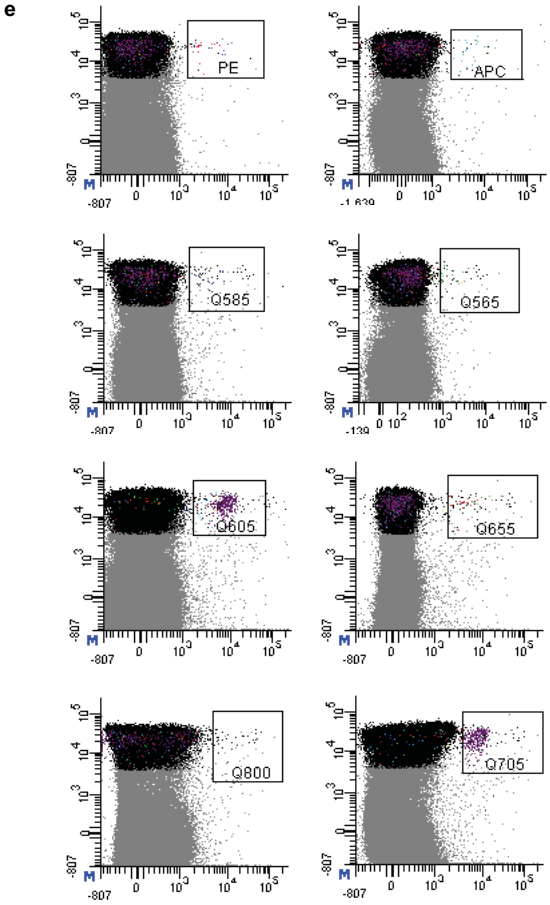

Supplementary Figure 3
Feasibility of 3D pMHC multimer staining

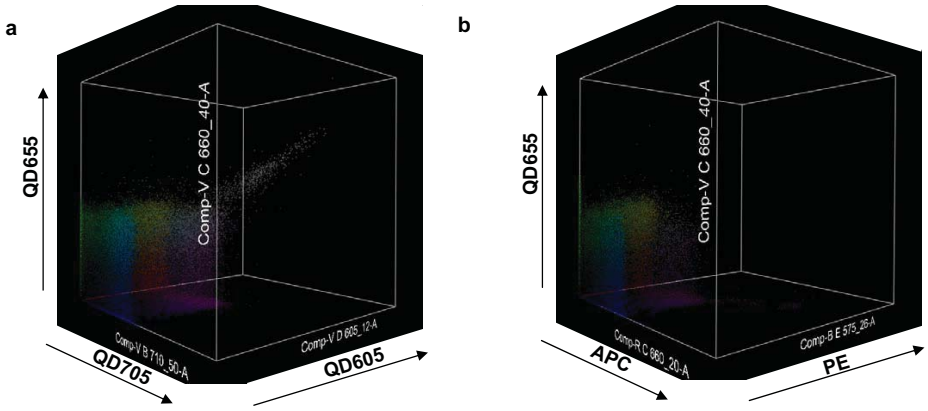

CMV_{NLV}–specific T cells are stained with a combination of QD605, QD655 and QD705 labeled CMV_{NLV}–MHC multimers. **(a)** The parameters QD605, QD655 and QD705, with the triple positive cells in white. **(b)** The parameters PE, APC and QD655 of the same sample. No triple positive cells were detected using this combination. 3D dot plots were made using FlowJo v7.5 (beta version).

Supplementary Figure 4

Phenotypic characterization of virus–specific T cells detected by combinatorial encoding

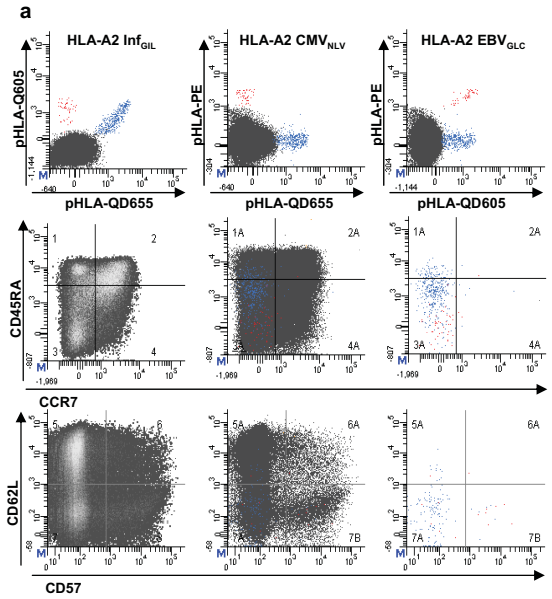

(**a–c**) dot plots from three healthy donors gated on approximately 200,000 CD8$^+$ T cells after exclusion of 'triple' or 'single' pMHC multimer positive T cells. (**top row**) PBMCs were stained with pMHC–multimer complexes for HLA–A2 Inf$_{GIL}$ (QD605 + QD655, blue), HLA–A2 CMV$_{NLV}$ (PE + QD655, green), and HLA–A2 EBV$_{GLC}$ (PE + QD605, red). (**middle row**) Phenotypic characteristics of virus–specific T cells based on CD45RA and CCR7 expression: a density plot gated on CD8$^+$ T cells used to define quadrant gates (left), a dot plot showing all CD8$^+$ T cells with pMHC positive T cells depicted in the indicated colors (middle), and a dot plot showing only pMHC positive T cells (right). (**bottom row**) Phenotypic characteristics of virus–specific T cells based on CD62L and CD57 expression: a density plot gated on CD8$^+$ T cells used to define quadrant gates (left), a dot plot showing all CD8$^+$ T cells with pMHC positive T cells depicted in the indicated colors (middle), and a dot plot showing only pMHC positive T cells (right).

Supplementary Figure 4

Phenotypic characterization of virus–specific T cells detected by combinatorial encoding

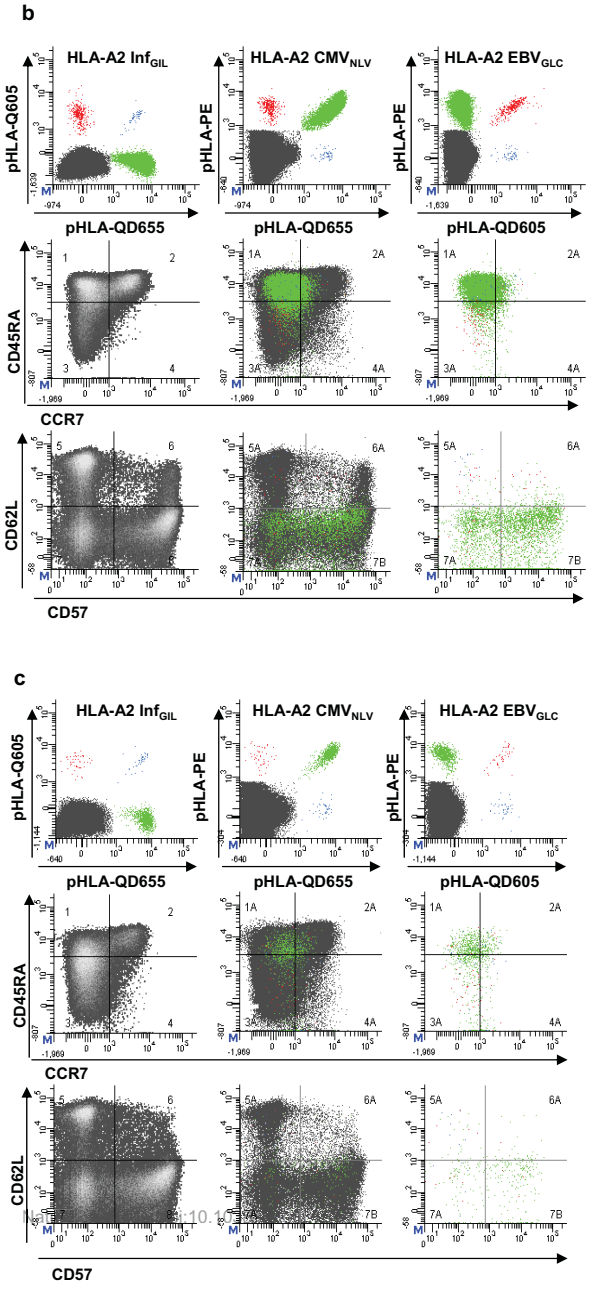

Supplementary Table 1

The 28 unique color combinations that can be made using a two–dimensional matrix of eight fluorochromes

	PE	APC	QD565	QD585	QD605	QD655	QD705	QD800
PE		x	x	x	x	x	x	x
APC			x	x	x	x	x	x
QD565				x	x	x	x	x
QD585					x	x	x	x
QD605						x	x	x
QD655							x	x
QD705								x
QD800								

Supplementary Table 2
Virus–derived and cancer–associated T cell epitopes

No.	Protein	HLA Restriction	Peptide	Coding
1	*HPV E6*	A2	TIHDIILECV	PE & APC
2	*CMV pp150*	A3	TTVYPPSSTAK	PE & Q565
3	*Influenza A M1*	A2	GILGFVFTL	PE & Q585
4	*gp100*	A2	IMDQVPFSV	PE & Q605
5	*EBV LMP2*	A2	CLGGLLTMV	PE & Q655
6	*EBV BMF1*	A2	GLCTLVAML	PE & Q705
7	*Tyrosinase*	A2	YMNGTMSQV	PE & Q800
8	*Survivin*	A2	LMLGEFLKL	APC & Q565
9	*CMV pp65*	A1	YSEHPTFTSQY	APC & Q585
10	*EBV LMP2*	A2	FLYALALLL	APC & Q605
11	*Influenza A NP*	A3	ILRGSVAHK	APC & Q655
12	*HA-2*	A2	YIGEVLVSV	APC & Q705
13	*CMV pp65*	A2	NLVPMVATV	APC & Q800
14	*CMV pp65*	B7	TPRVTGGGAM	Q565 & Q605
15	*CMV pp50*	A1	VTEHDTLLY	Q565 & Q655
16	*EBV BRLF1*	A2	YVLDHLIVV	Q565 & Q705
17	*HPV E7*	A2	YMLDLQPETT	Q585 & Q605
18	*EBV EBNA 3a*	A3	RLRAEAQVK	Q585 & Q655
19	*Influenza A BP1*	A1	VSDGGPNLY	Q585 & Q705
20	*CMV pp65*	B7	RPHERNGFTV	Q605 & Q655
21	*EBV EBNA*	B7	RPPIFIRLL	Q605 & Q705
22	*HY*	A2	FIDSYICQV	Q605 & Q800
23	*CMV pp150*	A3	TVYPPSSTAK	Q655 & Q705
24	*CMV IE1*	A2	VLEETSVML	Q655 & Q800
25	*EBV BRLF1*	A3	RVRAYTYSK	Q705 & Q800

For each epitope MHC multimers were encoded by the indicated fluorochrome combination

Supplementary Table 3
Melanoma–associated HLA–A3 ligands

Protein	Peptide	Position	Coding
Gp100	**IALNFPGSQK**	86-95	PE & APC
	LIYRRRLMK	614-622	PE & Q565
	GTATLRLVK	460-468	PE & Q585
	ALLAVGATK	17-25	PE & Q605
	ALNFPGSQK	87-95	PE & Q655
	GVSRQLRTK	34-42	PE & Q705
	QLVLHQILK	551-559	PE & Q800
	QLRALDGGNK	221-230	APC & Q565
Nodal	SLYRDPLPR	46-54	APC & Q585
	HAYIQSLLK	293-301	APC & Q605
	KTKPLSMLY	317-325	APC & Q655
	RVAGECWPR	175-183	APC & Q705
Tyr	YMVPFIPLYR	425-434	APC & Q800
	SLLCRHKRK	497-505	Q565 & Q605
	VSSKNLMEK	25-33	Q565 & Q655
	GLVSLLCRHK	494-503	Q565 & Q705
Tyrp1	SLPYWNFATR	245-254	Q585 & Q605
	ASYLIRARR	497-505	Q585 & Q655
Tyrp2	TLLGPGRPYR	196-205	Q585 & Q705
	GTYEGLLRR	301-309	Q605 & Q655
	RMYNMVPFF	461-469	Q605 & Q705
	VLLAFLQYR	521-529	Q605 & Q800
Influenza A NP	**ILRGSVAHK**	265-273	Q655 & Q705
EBV EBNA 3a	**RLRAEAQVK**	603-611	Q655 & Q800
EBV BRLF1	**RVRAYTYSK**	148-156	Q705 & Q800

Three EBV– and influenza A–derived epitopes were included for direct *ex–vivo* stainings as a positive control. Sequences in bold are previously described T cell epitopes. Individual pMHC multimers were encoded by the indicated fluorochrome combination.

Supplementary Table 4
HIV– and HCV–derived HLA–A3 restricted T cell epitopes

Virus	Peptide	Position	Coding
HIV	QVPLRPMTYK	86-95	PE & APC
HIV	TVYYGVPVWK	614-622	PE & Q565
HIV	RLRDLLLIVTR	460-468	PE & Q585
HIV	RLRPGGKKK	17-25	PE & Q605
HIV	KIRLRPGGK	87-95	PE & Q655
Hepatitis C virus	RVCEKMALY	34-42	PE & Q705
Hepatitis C virus	RLGVRATRK	551-559	PE & Q800
Hepatitis C virus	KTSERSQPR	221-230	APC & Q565
Hepatitis C virus	QLFTFSPRR	46-54	APC & Q585
Hepatitis C virus	RMYVGGVEHR	293-301	APC & Q605
Hepatitis C virus	LGFGAYMSK	317-325	APC & Q655
Hepatitis C virus	GAYMSKAHGV	175-183	APC & Q705
Hepatitis C virus	LIFCHSKKK	425-434	APC & Q800
Hepatitis C virus	GVAGALVAFK	497-505	Q565 & Q605
Hepatitis C virus	VAGALVAFK	25-33	Q565 & Q655
Hepatitis C virus	SLTPPHSAK	494-503	Q565 & Q705
Hepatitis C virus	CINGVCWTC	245-254	Q585 & Q605
Hepatitis C virus	HDGAGKRVY	497-505	Q585 & Q655
Hepatitis C virus	KVFPKALINK	196-205	Q605 & Q655
Hepatitis C virus	LLFLLLADA	301-309	Q605 & Q800
Influenza A NP	ILRGSVAHK	265-273	Q655 & Q705
EBV EBNA 3a	RLRAEAQVK	603-611	Q655 & Q800
EBV BRLF1	RVRAYTYSK	148-156	Q705 & Q800

Three EBV– and influenza A–derived epitopes were included for direct *ex–vivo* stainings as a positive control. Individual pMHC multimers were encoded by the indicated fluorochrome combination.